

Article

Influence of Waste Tire Particles on Freeze–Thaw Resistance and Impermeability Performance of Waste Tires/Sand-Based Autoclaved Aerated Concrete Composites

Chang Chen ^{1,*} , Ruyi Zhang ¹, Li Zhou ¹ and Yubin Wang ²

¹ College of Materials Science and Engineering, Xi'an University of Architecture and Technology, Xi'an 710055, China; cassie@xauat.edu.cn (R.Z.); zzhouli@xauat.edu.cn (L.Z.)

² School of Resources Engineering, Xi'an University of Architecture and Technology, Xi'an 710055, China; wywywyb@xauat.edu.cn

* Correspondence: changchen420@xauat.edu.cn

Abstract: Waste tires/sand-based autoclaved aerated concrete (SAAC) composites were prepared by mixing waste tires, which have different particle sizes and content. The physical performance, mechanical properties, freeze–thaw resistance, impermeability performance, phase composition, and microstructure of waste tires/sand-based autoclaved aerated concrete composite materials were examined. The results demonstrated that the 750- μm -sized waste tire particles on the surface of the SAAC composite did not agglomerate. Moreover, these particles did not damage the pore structure of the composites. The SAAC composites, with a relatively high compressive strength and low mass-loss rate, were obtained when the contents of waste tire particles ranged from 1.0 to 2.5 wt.%. For composites prepared with 2.0 wt.% of 750- μm -sized waste tire particles, the optimal compressive and flexural strength values were 3.20 and 0.95 MPa, respectively. The increase in the rate of water absorption on SAAC composites was lowest (i.e., 16.3%) when the soaking time was from 24 to 120 h.

Keywords: waste tire particles; sand-based autoclaved aerated concrete; mechanical properties; freeze–thaw resistance; impermeability performance



Citation: Chen, C.; Zhang, R.; Zhou, L.; Wang, Y. Influence of Waste Tire Particles on Freeze–Thaw Resistance and Impermeability Performance of Waste Tires/Sand-Based Autoclaved Aerated Concrete Composites.

Buildings **2022**, *12*, 33. <https://doi.org/10.3390/buildings12010033>

Academic Editors: Shengwen Tang and Lei Wang

Received: 8 December 2021

Accepted: 23 December 2021

Published: 1 January 2022

Publisher's Note: MDPI stays neutral with regard to jurisdictional claims in published maps and institutional affiliations.



Copyright: © 2021 by the authors. Licensee MDPI, Basel, Switzerland. This article is an open access article distributed under the terms and conditions of the Creative Commons Attribution (CC BY) license (<https://creativecommons.org/licenses/by/4.0/>).

1. Introduction

Large quantities of waste tires from the rapidly growing automobile and rubber industries has caused environmental concerns [1,2]. These concerns are present in multiple countries, and thus the sustainable management of waste tires must be developed [3,4]. A possible solution is to incorporate waste tires into concrete [1,5,6]. The resulting product may be used to replace concrete with mineral aggregates that are used for various purposes. For example, rubberized concrete has received considerable attention as a type of new building material [7–9]. The effects of waste tires on the physical properties and durability of ordinary concrete have been performed in multiple studies. Li et al. [10] examined the effects of steel fiber and rubber particles on the mechanical properties and seismic behavior of high-strength concrete. Rubber particles improved the compressive strength and toughness of the concrete. Ganjian et al. [11] demonstrated that rubber was able to decrease the water permeability depth of concrete. The water absorption decreased when the coarse aggregate was replaced by waste tire rubber. Basic et al. [12] demonstrated that rubber-recycled concrete had improved fracture energy and fracture toughness. The improvement was facilitated by the increase in the rubber replacement rate under the condition of a constant replacement rate of the recycled aggregate. The fatigue and impact resistance characteristics of waste rubber-recycled concrete were better than those of recycled concrete. The chloride ion permeability and freeze–thaw resistance of waste rubber-recycled concrete were enhanced by the increase in the rubber particle substitution rate. Yu et al. [13] examined the frost and thawing resistance of waste rubber-recycled concrete. They reported that

the frost resistance of waste rubber concrete was better than the control concrete. The frost and thawing resistance improved with the reduction in rubber particle size, and the best substitution ratio for the rubber aggregate was ~10%. Rubberized concrete has been utilized for many years. However, the sustainable management of large quantities of tire wastes is not yet well-developed [14–16]. Sand-based autoclaved aerated concrete (SAAC) is a new type of environmentally friendly building material with a porous structure, as well as soundproof and heat-resistant properties. In SAAC production, industrial solid wastes (e.g., waste tires, coal gangue, iron ore tailings, etc.) have been used as substitutes for natural materials. This was done to relieve the pressure of solid waste pollution and depletion of natural resources. However, the durability of SAAC has been reported to be poor compared to ordinary concrete [17–20]. Studies demonstrated that the carbonization, frost, and permeability resistance of SAAC were lower than that of ordinary concrete. The use of waste tire particles in SAAC composites will reduce natural resource demand in SAAC production and create a sustainable management strategy for waste tires [21–23]. Therefore, in this paper, the effect of waste tires with different particle sizes on the physical performance and mechanical properties of SAAC composites was conducted for the first time. The optimal waste tire particle size was determined for composites. The effects of waste tire particles on the freeze–thaw resistance and impermeability of the composites containing different amounts of waste tire particles were analyzed. X-ray diffraction (XRD) was used to determine the phase composition of composites. Scanning electron microscopy (SEM) was used to assess the morphology of the cross-sections of composites.

2. Materials and Methods

2.1. Materials

The Portland cement (P.O 42.5) used in the experiments was obtained from Tangshan Jidong Cement Co., Ltd., which complies with the regulations of GB 175 “Common Portland cement”. The initial and final setting times of the Portland cement were 170 and 230 min, respectively. Lime used in this study was natural limestone which was ground to required fineness. Calcium oxide meets the requirements of JC/T 621 “Lime for silicate building products”, with an effective content of 74.26%, a curing time of 13 min and a curing temperature of 97.5 °C. Gypsum was purchased from Shaanxi Huadian Pucheng Power Generation Co., Ltd., which complies with the regulations of JC/T 2074-2011 “Flue gas desulfurization gypsum”. Gypsum was mixed with water to form the gypsum slurry. Gypsum slurry has a density of $\sim 1.5 \times 10^3 \text{ kg/m}^3$. The sand slurry was mixed with tailings sand (from a glass factory) and tap water. The sand slurry conforms to JC/T 622 “Sand for silicate building products”. The quartz content of the tailings sand was 93%. Waste slurry was prepared by mixing ground SAAC waste blocks and water. The activity of Al powder was 94%, which complies with GB/T 2085.2 “Aluminum powder Part 2: Inflammable fine aluminum powder”. Three different particle sizes of waste tire were used in this study. Figure 1 shows the representative images of waste tires.

2.2. Preparation of the Waste Tires/Sand-Based Autoclaved Aerated Concrete Composites

The SAAC samples were prepared as per GB/T 11968-2020 “Autoclaved aerated concrete blocks” method. As per Table 1, the slurry was prepared by mixing sand, waste, and gypsum slurries. Portland cement, lime, and waste tires were added into the slurry and then stirred for 2 min. An appropriate amount of Al powder was added to the mixed slurry (to make 0.069 wt.% Al powder compared to the slurry). The mixture was stirred for 40 s before pouring into the molds. The SAAC samples were obtained by curing at 190 °C and 1.2 MPa.

The B05 SAAC samples with 1.0 wt.% waste tires were obtained because the ordinary concrete containing 1.0 wt.% waste tire provided better performance than the ordinary concrete without waste tire [24]. Therefore, the samples with the size of 100 mm × 100 mm × 100 mm were prepared in the factory by three different types (waste tire content was 1.0%, and waste tire particle size were 2 mm, 750 μm, 375 μm respectively). Ten samples were prepared for each

size of each type of waste tire/sand aerated concrete composite. The performance of SAAC samples prepared with different particle sizes of waste tire was investigated. Table 2 shows the particle sizes (I, II and III) of waste tires in the SAAC samples. The optimal particle size was selected by preparing waste tires with different contents (i.e., 0.5–3.0 wt.% in 0.5 wt.% increments). Ten samples were prepared for each size of each type and the performance of SAAC samples prepared with different content of waste tires was investigated.

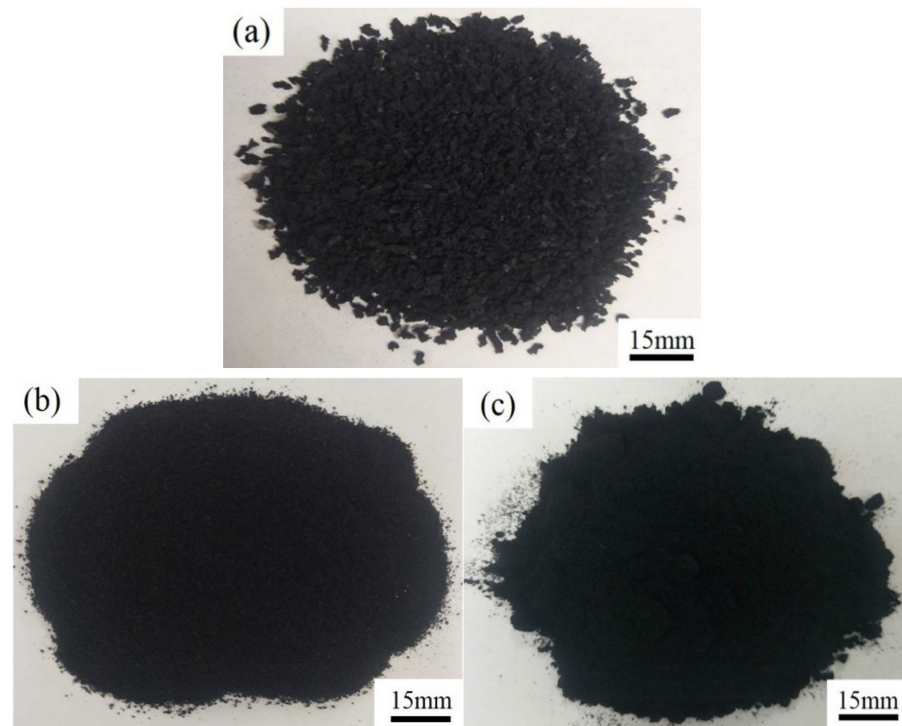


Figure 1. Representative images of the waste tires having different particle sizes ((a) 2 mm, (b) 750 μm , and (c) 375 μm).

Table 1. The mixing ratio of B05 SAAC samples.

Raw Materials	Sand Slurry	Waste Slurry	Gypsum Slurry	Portland Cement	Lime
Content/wt.%	47.00	20.00	3.00	17.00	13.00

Table 2. The particle sizes of waste tires used in the SAAC samples.

Samples	Particle Sizes of Waste Tires	Waste Tire Content
I	2 mm	
II	750 μm	1.0 wt.%
III	375 μm	

2.3. Test Methodology

The compressive and flexural strength of samples were tested by cement mortar flexural compressive tester as per GB/T 11968-2020. The freeze–thaw resistance and impermeability tests were carried out as per GB/T 11968-2020 by using electric heating air-blast drying oven, constant temperature water tank and freezer. The compressive strength values of SAAC samples containing waste tires were analyzed through five freeze–

thaw cycles. The mass-loss rate was measured by weighing the samples under thawing conditions. The mass-loss rate of samples was calculated by Equation (1):

$$M_m = \frac{M_o - M_s}{M_o} \times 100\% \quad (1)$$

where M_m is the mass-loss rate (%), M_o is the mass of samples before the freeze–thaw test (g), and M_s is the mass of samples after the freeze–thaw test (g). The samples were placed in an impermeable test facility and soaked for 24 h through addition of water to 1/3 height of samples. Moreover, the above procedures were repeatedly performed when the height of added water were 2/3 height of the samples and 30 mm higher than the height of the samples, respectively. The samples were collected and wiped with a damp cloth before they were weighed. The phase composition of the SAAC samples was measured using a Rigaku D/max-III A X-ray diffractometer (CuK α wavelength = 1.5406 nm, scanning step = 0.02 at 10°/min from 0° to 90°) from Shimadzu enterprise management [China] Co., Ltd. The microstructures of the samples were examined using SEM (Quanta 200, FEI company, Hillsboro, OR, USA). The cut cuboid samples with the size of 4 mm \times 4 mm \times 10 mm were dried in an electric blast drying oven. The dried samples were dispersed with anhydride. After spraying gold, the morphology is observed under the scanning electron microscope with different magnification rates. SEM was used to investigate the section morphology of samples.

3. Results and Discussion

3.1. Effect of the Particle Size of Waste Tires on Physical Performance and Mechanical Properties of SAAC

Figure 2 shows the images of the surfaces of SAAC samples with 2 mm, 750 μ m, and 375 μ m waste tire particles. The 2 mm particles were unevenly dispersed in the samples (Figure 2a). These particles were reported on the surface of the SAAC sample. The 750- μ m-sized waste tire particles did not agglomerate and were evenly dispersed on the surface of the SAAC sample (Figure 2b). A large number of empty spots appeared on the surface of the sample with the 375- μ m-sized waste tire particles (Figure 2c). This suggested that the 375 μ m waste tire particles added to the SAAC sample fill a small part of the pores, resulting in a large number of empty spots on the sample surface.

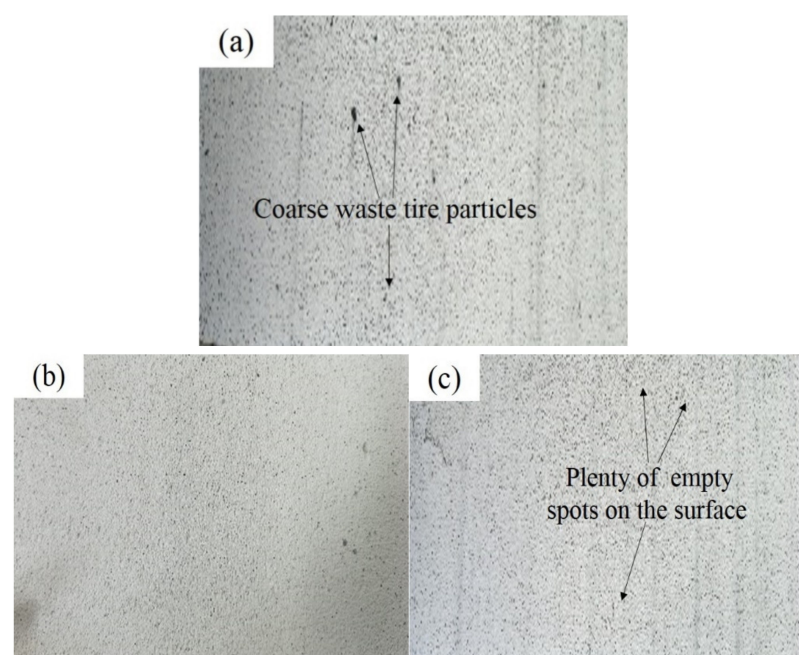


Figure 2. (a–c) are samples with 2 mm, 750 μ m, and 375 μ m waste tire powder, respectively.

Figure 3 shows the variation of slump flow, dry density, and compressive strength of the SAAC samples with the different particle sizes of waste tires. The slump flow values of the slurry increased and then decreased with the decreasing of the particle sizes of the waste tires. The effect of 750- μm -sized particles on the slump flow of the slurry was optimal for three types of waste tires, and the slump flow value was 360 mm. The dry density values were not affected by the particle size. The maximum and minimum values were 528 and 499 kg/m^3 , respectively. These values met the dry density requirements of B05 SAAC in the GB/T 11968-2020 “Autoclaved aerated concrete blocks”.

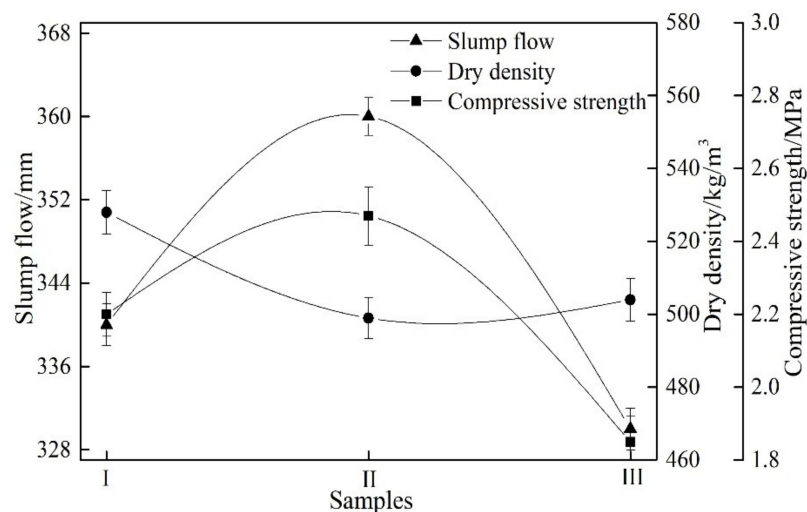


Figure 3. Slump flow, dry density, and compressive strength of the SAAC samples with different particle sizes of waste tires. I, II, III samples were 2 mm, 750 μm , 375 μm , respectively.

The compressive strength values of SAAC samples increased first and then decreased with the decrease in the particle size. The optimal compressive strength value of 2.47 MPa was obtained when 750- μm -sized particles were added. According to GB/T 11968-2020 “Autoclaved aerated concrete blocks”, B05 SAAC compressive strength 2.47 MPa meets the grade requirements of B05 SAAC. Since the pore sizes of the SAAC composites ranged from 0.5 to 1.5 mm [24], therefore, the 750- μm -sized particles were suitable for the pore sizes of SAAC composites. This resulted in the improved compressive strength of composites [25]. The 750- μm -sized waste particles filled the pores, thereby protecting the pore structure of the SAAC.

3.2. Effect of 750- μm -Sized Waste Tire Content on the Physical Performance and Mechanical Properties of SAAC

Figure 4 shows the slump flow and dry density of the SAAC samples with different content of 750- μm -sized waste tire particles. The slump flow values of the slurry were unchanged (~ 350 mm) when the amount of waste tire added to the SAAC sample increased from 0.5 to 3.0 wt.%. The dry density values of the samples were ~ 500 kg/m^3 .

Figure 5 shows the compressive strength and flexural strength of the samples with different waste tire contents. In general, the compressive strength of the samples increased and then decreased with the increase of waste tire content. The spacings between the particles changed when the waste tires content was modified in the SAAC composites. The spacings between the particles were wide when the content was low. On the other hand, the spacings were narrow when the content was high [26]. The pore structures of the SAAC were easily destroyed in both cases (low and high content). This led to a decrease in the compressive and flexural strength of the composites [13,27]. Therefore, when the waste tire content was 2.0 wt.%, the compressive strength (3.20 MPa) of the SAAC samples was the highest. The flexural strength values of the samples gradually increased with an increase in the waste tire content. The values then decreased when the waste tire content

ranged from 2.0 to 3.0 wt.%. When the waste tire content was 2.0 wt.%, the flexural strength reached the optimal value of 0.95 MPa. However, the flexural strength of the samples that contained >2.0 wt.% of the particles decreased because of the damage of pore structures of the samples [28–30].

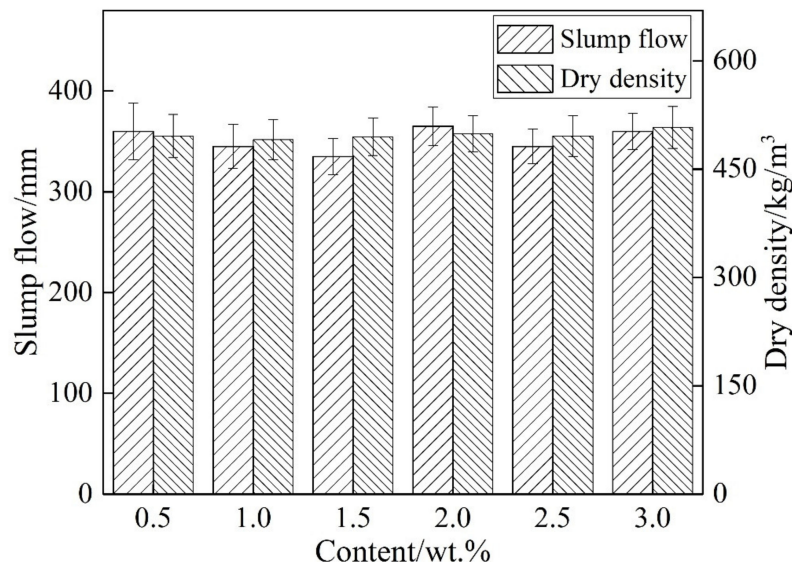


Figure 4. Slump flow and dry density of the SAAC samples with different content of 750 μm waste tire particles.

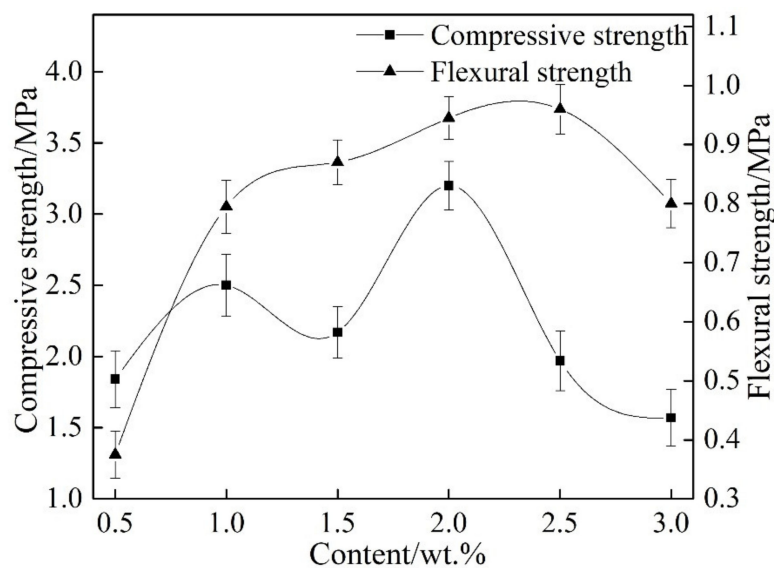


Figure 5. Compressive strength and flexural strength of the SAAC samples with different content of waste tire particles.

3.3. Effect of 750 μm Waste Tire Particles Content on the Frost Resistance of SAAC

The relative compressive strength and mass-loss rate of the SAAC samples containing waste tire particles during five freeze–thaw cycles were studied, and the results are shown in Figure 6. When 0.5 wt.% of waste tire particles were added, the relative compressive strength was 59.8%, and the mass-loss rate was 13.2%. The internal open pores of the samples were blocked during the mixing with waste tires particles. The material can then be potentially destroyed by the expansion of gas within the pores, thus affecting the quality of the SAAC [31,32]. When the additive content increased from 1.0 to 2.5 wt.%, the relative compressive strength gradually increased. The relative compressive strength

values of these samples were slightly lower than that of samples with 1.0 wt.% particles. This was consistent with a result from the mass-loss rate experiments, particularly when the content of the particles was 1.5 wt.%. Moreover, the mass-loss rate values of the samples containing 750- μm -sized particles were low when the content was from 1.0 to 2.5 wt.%. A certain number of particles could be evenly distributed into the samples. Better stability and performance are achieved when pores in the sample were filled with particles [33]. Moreover, the water content in the abovementioned samples was lower than that in the sample containing 0.5 wt.% particles. The pressure generated during the formation of ice will be lower in these samples [34,35]. Nevertheless, the waste tire particles are the elastic materials, and thus the free water in the B05 SAAC samples froze and the waste tire distributed in the pores deformed to resist the volumetric expansion pressure of ice during the freeze–thaw cycle. Therefore, the addition of waste tire particles could potentially improve the frost resistance of the SAAC samples [36]. However, when the particle content was 3.0 wt.%, the relative compressive strength of the SAAC samples was low. The mass-loss rate value of 10.6% was high. The excess waste tire particles would enter the matrix of the B05 SAAC samples and produce a large number of weak waste tire–sand aerated concrete interface, which destroyed the pore structure of sand aerated concrete, so the relative compressive strength of the samples decreased and the mass-loss rate of the samples increased [37]. Therefore, when the amounts of waste tire particles were from 1.0 to 2.5 wt.%, the frost resistance of the SAAC samples was optimal.

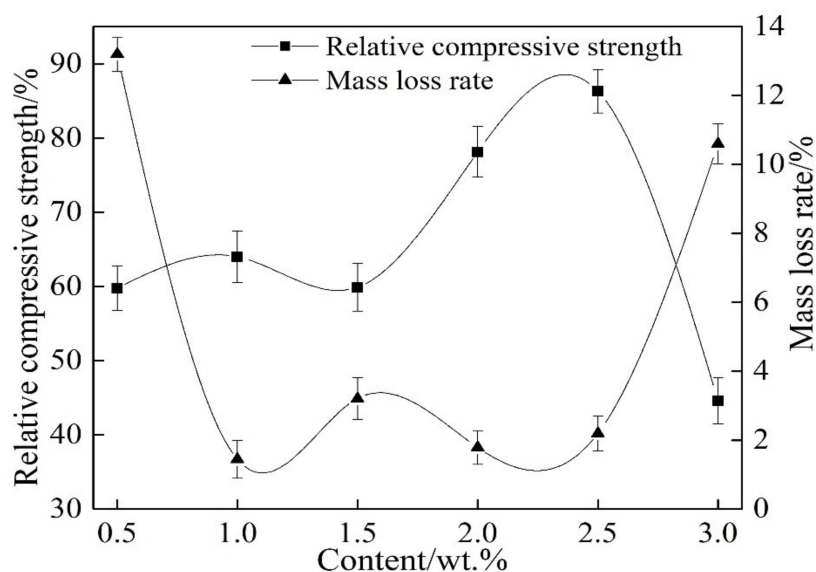


Figure 6. Relative compressive strength and mass-loss rate of the SAAC samples with different content of 750 μm waste tire particles.

3.4. Effect of 750 μm Waste Tire Particles Content on Impermeability Performance of SAAC

Figure 7 shows the impermeability results for the SAAC samples. The water absorption rate values obtained for the samples containing 0.5, 1.5, and 3.0 wt.% particles were significantly higher than those containing 1.0, 2.0, and 2.5 wt.% particles (24 h soaking time). The value (50.5%) was lowest in the sample containing 2.5 wt.% particles. However, when the soaking time for the 2.0 wt.% sample increased from 24 to 120 h, the rate was extremely low, or 16.3%. When the particles are evenly dispersed in the matrix, blockage of the capillary channels was most likely to occur because of the particles in the samples [34]. Waste tire powder contained a hydrophobic polymer material and could form a layer of hydrophobic membrane on the surface. This powder could be used to decrease the penetration of water and reduce the surface tension of capillary pores [35,38]. Thus, we concluded that the impermeability of the SAAC sample was optimal when the content of the 750- μm -sized waste tire particles was 2.0 wt.%.

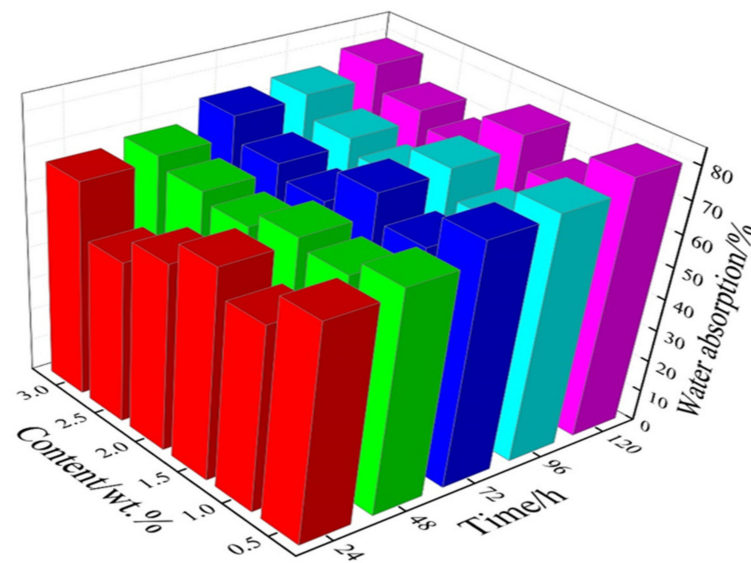


Figure 7. Water absorption of the SAAC samples with different content of 750 μm waste tire particles.

3.5. Effect of 750 μm Waste Tires Particles Content on the Microstructure of SAAC

Figure 8 shows the XRD patterns of samples with different waste tire content. Table 3 lists the effect of relative contents on the phase compositions in the XRD patterns. The phases of silicon dioxide, tobermorite, and calcium silicate hydrate were characterized in samples with waste tire content ranging from 0.5 to 3.0 wt.%. Different raw materials were used to prepare the SAAC samples; however, no changes in the chemical composition were observed in these samples. Therefore, the addition of 750- μm -sized waste tire particles had no effect on the phase composition of the SAAC. However, as shown in Table 3, the relative mass percentage of silicon dioxide, tobermorite, and calcium silicate hydrate changed. The content of silicon dioxide and calcium silicate in the SAAC samples gradually decreased; however, the content of tobermorite gradually increased with the increase in the particles' content. In addition, the increment of tobermorite was higher than the decrement of silicon dioxide. The tobermorite content affected the strength of the SAAC, where the higher content of tobermorite increased the strength of the samples [30]. When the waste tire content was 2.0 wt.%, the relative mass percentage of silicon dioxide and tobermorite was 53 and 36 wt.%, respectively. When the waste tire contents were 2.5 and 3.0 wt.%, the relative mass percentages of tobermorite were 41 and 43 wt.%, respectively. Although the amounts of tobermorite in the samples containing 2.5 and 3.0 wt.% waste tire particles were higher than that of the sample containing 2.0 wt.% waste tire particles, for the formers, the excess particles in the matrix reduced the strength of the SAAC with 2.0% particles. Therefore, the strength of the samples with 2.5 and 3.0 wt.% particles was lower than the samples with 2.0 wt.% particles.

Figure 9 shows the SEM images of SAAC samples mixed with 750- μm -sized waste tire particles. Figure 9a,b,d,e show the pore sizes in the section of the SAAC samples mixed with 0.5, 1.0, 2.0, and 2.5 wt.% of 750- μm -sized, respectively. The pore size of each sample was ~ 1.0 mm. The images show integrated smooth pores and dense pore walls. It was observed that the tobermorite crystals in these pores were evenly distributed. The crystals have fine and regular needle-like morphology (see 2000 \times magnification in the figures). The water absorption of SAAC samples was related to the distribution uniformity, size, and connectivity of pores [39,40]. Thus, the composites demonstrated poor water absorption and high impermeability characteristics. The pore structure and inherent physical characteristics of the tobermorite crystals have a significant influence on the strength and mass-loss of SAAC [41]. These favor the frost resistance of the SAAC composites [26]. However, the measured pore size for the samples containing 1.5 and 3.0 wt.% particles was 2.0 mm (see Figure 9c,f). From the 2000 \times magnification results shown in Figure 9c,f, the diameter of the

inner walls of the pores were large, and the crystals were rough and disorderly. Therefore, the impermeability and frost resistance of the samples were poor when 1.5 and 3.0 wt.% particles were added. Based on these results, the optimal content was 2.0 wt.% particles.

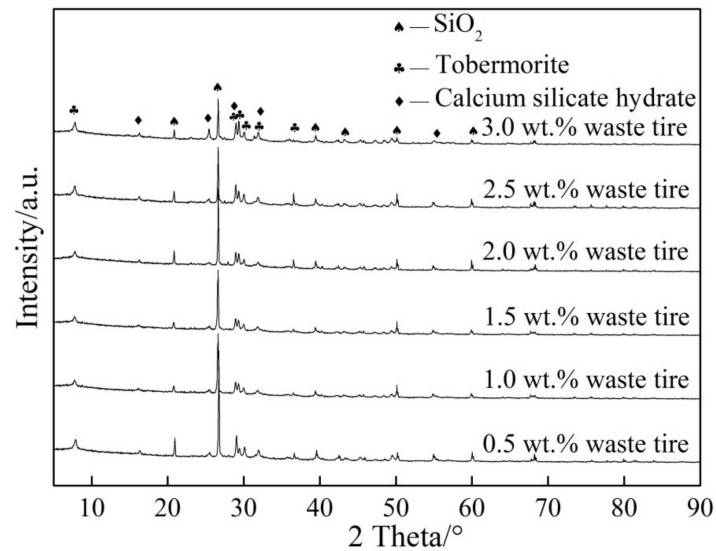


Figure 8. XRD patterns of SAACs that contained different amounts of 750 mm waste tire particles.

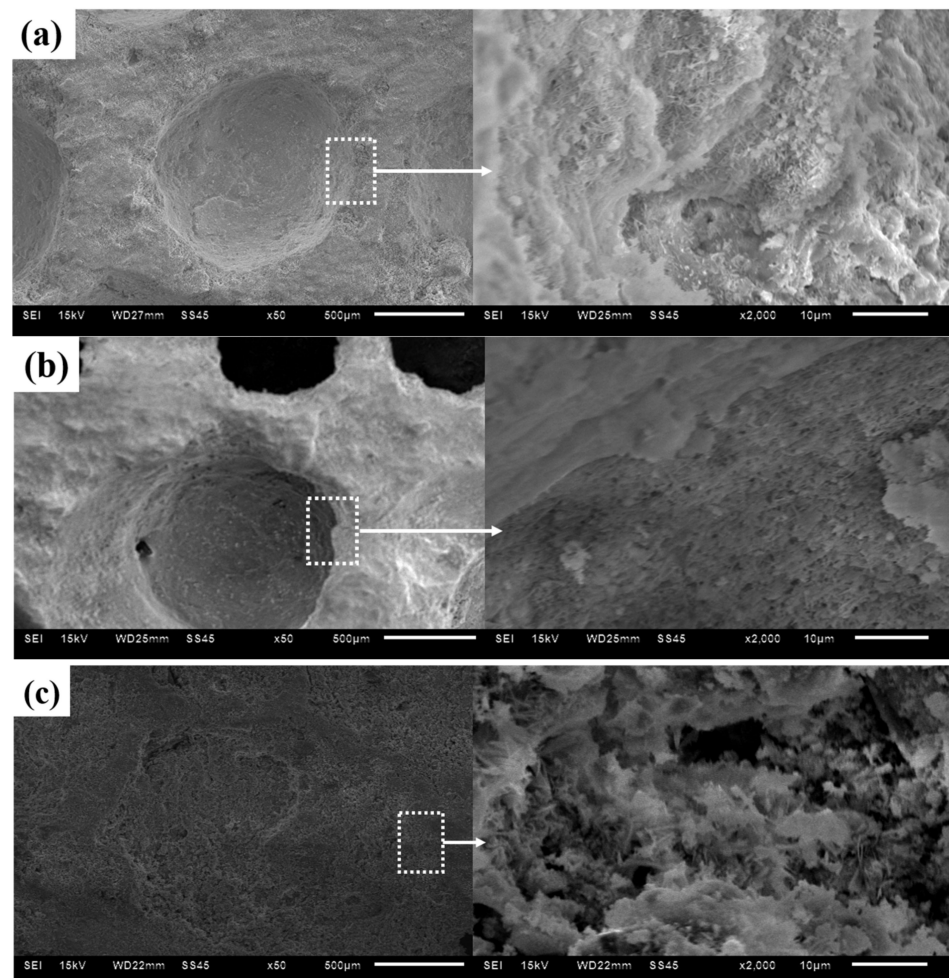


Figure 9. Cont.

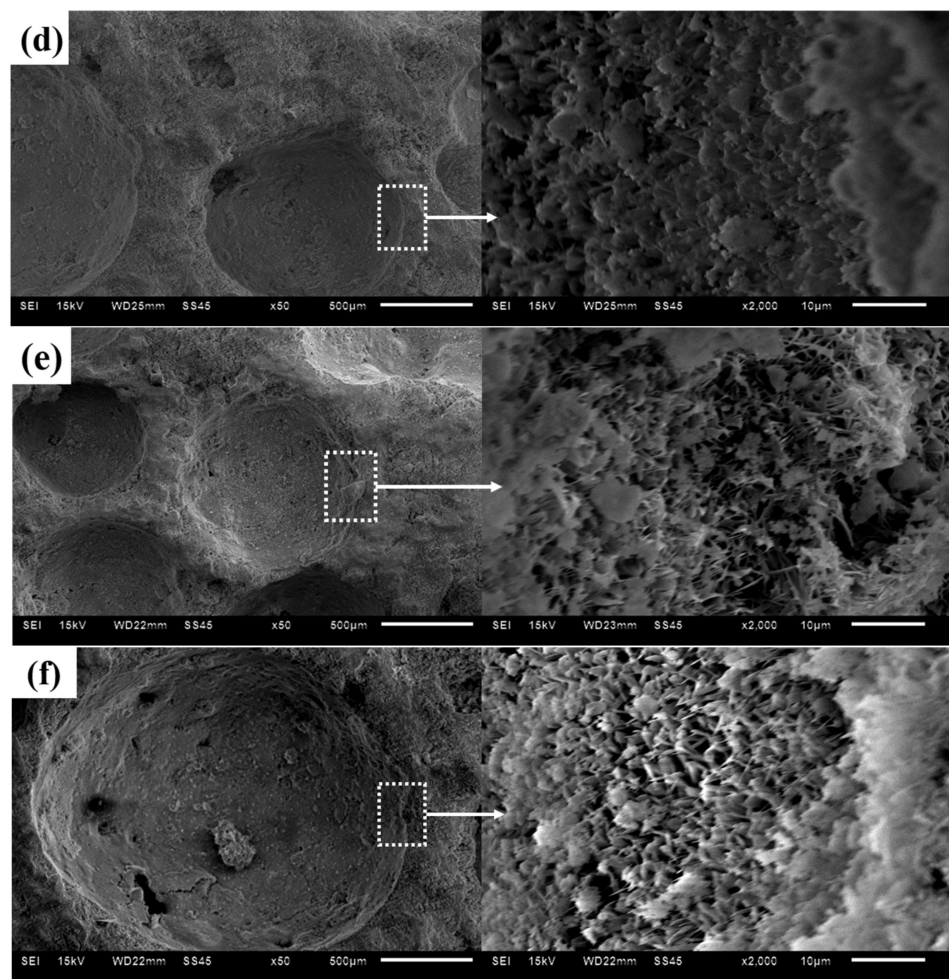


Figure 9. SEM images of SAAC with different amounts of 750- μ m-sized waste tire particles. (a–f) were obtained from 0.5, 1.0, 1.5, 2.0, 2.5, and 3.0 wt.% particles, respectively.

Table 3. Specific content of phase composition in the XRD pattern of SAAC samples.

Waste Tire Content/wt.%	0.5	1.0	1.5	2.0	2.5	3.0
silicon dioxide/wt.%	58	54	53	53	52	48
tobermorite/wt.%	16	25	33	36	41	43
calcium silicate hydrate/wt.%	26	21	14	11	7	9

4. Conclusions

In this study, the waste tire particles with the size of 750 μ m were evenly distributed on the surface of SAAC composite. The pore structure damage of SAAC composite was low. Particles do not agglomerate, and the pores of the composite were filled by particles, so 750- μ m-sized waste tire particles were the optimal particle size of SAAC composite. The influence of different content of 750 μ m waste tire particles on SAAC composite was studied. It was found that the compressive strength and flexural strength were optimal when the waste tire particle content was 2.0 wt.%. The values of strength were 3.20 MPa and 0.95 MPa, respectively. The pore sizes of the SAAC composites with 2.0 wt.% of 750- μ m-sized waste tire particles were \sim 1.0 mm. The tobermorite crystals were evenly distributed and had a fine and regular needle-like morphology. Thus, the water absorption was lowered, and the impermeability of the materials was improved. The pore structure and physical characteristics of tobermorite crystals have a considerable influence on the strength and mass-loss of composites. These crystals favored the frost resistance of SAAC composites.

Author Contributions: Conceptualization, C.C.; methodology, C.C.; validation, R.Z.; formal analysis, C.C., R.Z. and L.Z.; investigation, L.Z.; resources, C.C.; data curation, C.C.; writing—original draft preparation, R.Z.; writing—review and editing, C.C.; supervision, C.C.; project administration, Y.W. and C.C.; funding acquisition, Y.W. All authors have read and agreed to the published version of the manuscript.

Funding: This research was supported by the National Natural Science Foundation of China (No. 51974218).

Data Availability Statement: The data used to support the findings of this study are available from the corresponding author upon request.

Conflicts of Interest: The authors declare no conflict of interest.

References

1. Gupta, T.; Siddique, S.; Sharma, R.K.; Chaudhary, S. Behaviour of waste rubber powder and hybrid rubber concrete in aggressive environment. *Constr. Build. Mater.* **2019**, *217*, 283–291. [[CrossRef](#)]
2. Son, K.S.; Hajirasouliha, I.; Pilakoutas, K. Strength and deformability of waste tyre rubber-filled reinforced concrete columns. *Constr. Build. Mater.* **2011**, *25*, 218–226. [[CrossRef](#)]
3. Mendis, A.S.M.; Al-Deen, S.; Ashraf, M. Effect of rubber particles on the flexural behaviour of reinforced crumbed rubber concrete beams. *Constr. Build. Mater.* **2017**, *154*, 644–657. [[CrossRef](#)]
4. Gesoglu, M.; Güneyisi, E.; Hansu, O.; Ipek, S.; Asaad, D.S. Influence of waste rubber utilization on the fracture and steel-concrete bond strength properties of concrete. *Constr. Build. Mater.* **2015**, *101*, 1113–1121. [[CrossRef](#)]
5. Youssf, O.; Mills, J.E.; Hassanli, R. Assessment of the mechanical performance of crumb rubber concrete. *Constr. Build. Mater.* **2016**, *125*, 175–183. [[CrossRef](#)]
6. Bandarage, K.; Sadeghian, P. Effects of long shredded rubber particles recycled from waste tires on mechanical properties of concrete. *J. Sustain. Cem.-Based Mater.* **2020**, *9*, 50–59. [[CrossRef](#)]
7. Han, Q.; Wang, N.; Zhang, J.; Yu, J.; Hou, D.; Dong, B. Experimental and computational study on chloride ion transport and corrosion inhibition mechanism of rubber concrete. *Constr. Build. Mater.* **2021**, *268*, 121105. [[CrossRef](#)]
8. Záleská, M.; Pavlík, Z.; Cítek, D.; Jankovský, O.; Pavlíková, M. Eco-friendly concrete with scrap-tyre-rubber-based aggregate—Properties and thermal stability. *Constr. Build. Mater.* **2019**, *225*, 709–722. [[CrossRef](#)]
9. Xu, J.; Yao, Z.; Yang, G.; Han, Q. Research on crumb rubber concrete: From a multi-scale review. *Constr. Build. Mater.* **2020**, *232*, 117282. [[CrossRef](#)]
10. Li, Y.; Li, Y. Experimental study on performance of rubber particle and steel fiber composite toughening concrete. *Constr. Build. Mater.* **2017**, *146*, 267–275. [[CrossRef](#)]
11. Ganjian, E.; Khorami, M.; Maghsoudi, A.A. Scrap-tyre-rubber replacement for aggregate and filler in concrete. *Constr. Build. Mater.* **2009**, *23*, 1828–1836. [[CrossRef](#)]
12. Basic, R.; Milicevic, I.; Sipos, T.K.; Strukar, K. Recycled rubber as an aggregate replacement in self-compacting concrete—Literature overview. *Materials* **2018**, *11*, 1729. [[CrossRef](#)]
13. Yu, Q.; Yang, C.F.; Ye, W.C. Experimental study on frost-resistance property of waste rubber aggregate concrete. *Appl. Mech. Mater.* **2013**, *275*, 2055–2058. [[CrossRef](#)]
14. Karger-Kocsis, J.; Meszaros, L.; Barany, T. Ground tyre rubber (GTR) in thermoplastics, thermosets, and rubbers. *J. Mater. Sci.* **2013**, *48*, 1–38. [[CrossRef](#)]
15. Li, X.; Ling, T.C.; Mo, K.H. Functions and impacts of plastic/rubber wastes as eco-friendly aggregate in concrete—A review. *Constr. Build. Mater.* **2020**, *240*, 117869. [[CrossRef](#)]
16. Gregori, A.; Castoro, C.; Marano, G.C. Strength reduction factor of concrete with recycled rubber aggregates from tires. *J. Mater. Civil. Eng.* **2019**, *31*, 04019146. [[CrossRef](#)]
17. Yang, K.H.; Lee, K.H. Tests on high-performance aerated concrete with a lower density. *Constr. Build. Mater.* **2015**, *74*, 109–117. [[CrossRef](#)]
18. Koutny, O.; Kratochvil, J.; Opravil, T. Preparation of ultra-low volume weight autoclaved aerated concrete. *Ceram. Silikáty* **2017**, *61*, 45–51. [[CrossRef](#)]
19. Yang, F.; Liang, X.; Zhu, Y.; Wang, C.; Cui, X. Preparation of environmentally friendly and energy-saving autoclaved aerated concrete using gold tailings. *J. N. Mat. Electr. Sys.* **2019**, *22*, 159–164. [[CrossRef](#)]
20. Hang, M.; Cui, L.; Wu, J.; Sun, Z. Freezing-thawing damage characteristics and calculation models of aerated concrete. *J. Build. Eng.* **2020**, *28*, 101072. [[CrossRef](#)]
21. Mendis, A.S.M.; Al-Deen, S.; Ashraf, M. Behaviour of similar strength crumbed rubber concrete (CRC) mixes with different mix proportions. *Constr. Build. Mater.* **2017**, *137*, 354–366. [[CrossRef](#)]
22. Yung, W.H.; Yung, L.C.; Hua, L.H. A study of the durability properties of waste tire rubber applied to self-compacting concrete. *Constr. Build. Mater.* **2013**, *41*, 665–672. [[CrossRef](#)]

23. Drochytka, R.; Zach, J.; Korjenic, A.; Hroudová, J. Improving the energy efficiency in buildings while reducing the waste using autoclaved aerated concrete made from power industry waste. *Energy Build.* **2013**, *58*, 319–323. [[CrossRef](#)]
24. Chen, G.; Li, F.; Jing, P.; Geng, J.; Si, Z. Effect of pore structure on thermal conductivity and mechanical properties of autoclaved aerated concrete. *Materials* **2021**, *14*, 339. [[CrossRef](#)]
25. Wan, H.; Hu, Y.; Liu, G.; Qu, Y. Study on the structure and properties of autoclaved aerated concrete produced with the stone-sawing mud. *Constr. Build. Mater.* **2018**, *184*, 20–26. [[CrossRef](#)]
26. Perez, J.C.L.; Kwok, C.Y.; Senetakis, K. Effect of rubber size on the behaviour of sand-rubber mixtures: A numerical investigation. *Comput. Geotech.* **2016**, *80*, 199–214. [[CrossRef](#)]
27. Liu, Y.; Leong, B.S.; Hu, Z.T.; Yang, E.H. Autoclaved aerated concrete incorporating waste aluminum dust as foaming agent. *Constr. Build. Mater.* **2017**, *148*, 140–147. [[CrossRef](#)]
28. He, T.; Xu, R.; Chen, C.; Yang, L.; Yang, R.; Da, Y. Carbonation modeling analysis on carbonation behavior of sand autoclaved aerated concrete. *Constr. Build. Mater.* **2018**, *189*, 102–108. [[CrossRef](#)]
29. Liu, Q.; Singh, A.; Xiao, J.; Li, B.; Tamb, V.W.Y. Workability and mechanical properties of mortar containing recycled sand from aerated concrete blocks and sintered clay bricks. *Resour. Conserv. Recy.* **2020**, *157*, 104728. [[CrossRef](#)]
30. Lv, J.; Zhou, T.; Du, Q.; Wu, H. Effects of rubber particles on mechanical properties of lightweight aggregate concrete. *Constr. Build. Mater.* **2015**, *91*, 145–149. [[CrossRef](#)]
31. Angelin, A.F.; Andrade, M.F.F.; Bonatti, R.; Cecche Lintz, R.C.; Gachet-Barbosa, L.A.; Osório, W.R. Effects of spheroid and fiber-like waste-tire rubbers on interrelation of strength-to-porosity in rubberized cement and mortars. *Constr. Build. Mater.* **2015**, *95*, 525–536. [[CrossRef](#)]
32. Wang, L.; Li, G.; Guo, F.; Tang, S.; Xiao, L.; Hanif, A. Influence of reactivity and dosage of MgO expansive agent on shrinkage and crack resistance of face slab concrete. *Cem. Concr. Compos.* **2021**, *126*, 104333. [[CrossRef](#)]
33. Kunchariyakun, K.; Asavapisit, S.; Sinyoung, S. Influence of partial sand replacement by black rice husk ash and bagasse ash on properties of autoclaved aerated concrete under different temperatures and times. *Constr. Build. Mater.* **2018**, *173*, 220–227. [[CrossRef](#)]
34. Feng, L.; Yu, M.L.; Fang, N.G.; Juan, L.L. Fatigue performance of rubber-modified recycled aggregate concrete (RRAC) for pavement. *Constr. Build. Mater.* **2015**, *95*, 207–217.
35. Ding, G.X.; Yang, G.N.; Duan, W.H. Modification and application of waste rubber powder. *Asian J. Chem.* **2013**, *25*, 5790–5792. [[CrossRef](#)]
36. Herrera-Sosa, E.S.; Martínez-Barrera, G.; Barrera-Díaz, C.; Cruz-Zaragoza, E.; Ureña-Núñez, F. Recovery and modification of waste tire particles and their use as reinforcements of concrete. *Int. J. Polym. Sci.* **2015**, *2015*, 234690. [[CrossRef](#)]
37. Pacheco-Torgal, F.; Ding, Y.; Jalali, S. Properties and durability of concrete containing polymeric wastes (tyre rubber and polyethylene terephthalate bottles): An overview. *Constr. Build. Mater.* **2012**, *30*, 714–724. [[CrossRef](#)]
38. Wang, L.; Zeng, X.; Yang, H.; Lv, X.; Guo, F.; Shi, Y.; Hanif, A. Investigation and application of fractal theory in cement-based materials: A review. *Fractal Fract.* **2021**, *5*, 247. [[CrossRef](#)]
39. Wang, Y.; Huang, J.; Wang, D.; Liu, Y.; Zhao, Z.; Liu, J. Experimental study on hygrothermal characteristics of coral sand aggregate concrete and aerated concrete under different humidity and temperature conditions. *Constr. Build. Mater.* **2020**, *230*, 117034. [[CrossRef](#)]
40. Wang, Y.; Wang, W.; Wang, D.; Liu, Y.; Liu, J. Study on the influence of sample size and test conditions on the capillary water absorption coefficient of porous building materials. *J. Build. Eng.* **2021**, *43*, 103120. [[CrossRef](#)]
41. Sinica, M.; Sezeman, G.A.; Mikulskis, D.; Kligys, M. Impact of complex additive consisting of continuous basalt fibres and SiO₂ microdust on strength and heat resistance properties of autoclaved aerated concrete. *Constr. Build. Mater.* **2014**, *50*, 718–726. [[CrossRef](#)]